

# Studies on key enzyme(s) of leishmania parasite



Thesis submitted in the partial fulfillment for the  
Award of Degree

**Doctor of Philosophy**

By

*Preeti Ranjan*

SCHOOL OF BIOCHEMICAL ENGINEERING  
INDIAN INSTITUTE OF TECHNOLOGY  
(BANARAS HINDU UNIVERSITY)  
VARANASI - 221005  
INDIA

Roll No. 19011008

2024



# INDIAN INSTITUTE OF TECHNOLOGY (BHU)

VARANASI-221005

## CERTIFICATE

It is certified that the work contained in the thesis titled " *Studies on key enzyme(s) of leishmania parasite*" by "Preeti Ranjan" has been carried out under my supervision and that this work has not been submitted elsewhere for a degree. It is further certified that the student has fulfilled all the requirements of Comprehensive Examination, Candidacy and SOTA for the award of PhD degree.

Signature:

(Prof. Vikash Kumar Dubey)

Supervisor

School of Biochemical Engineering

Indian Institute of Technology (BHU) Varanasi

डा० विकास कुमार दुबे  
Dr. Vikash Kumar Dubey  
आचार्य  
Professor  
शैव रासायनिक अभियांत्रिकी स्कूल  
School of Biochemical Engineering  
भारतीय प्रौद्योगिकी संस्थान  
Indian Institute of Technology  
(काशी/वाराणसी), वाराणसी-221005  
(B.H.U.) Varanasi-221005



## COPYRIGHT TRANSFER CERTIFICATE

**Title of the Thesis:** Studies on key enzyme(s) of leishmania parasite

**Name of the Student:** Preeti Ranjan

### Copyright Transfer

The undersigned hereby assigns to the Institute of Technology (Banaras Hindu University) Varanasi all rights under copyright that may exist in and for the above thesis submitted for the award of the *Doctor of Philosophy*.

Date: 19/07/2024

Preeti Ranjan  
Signature of the Student:

Place: Varanasi

(Preeti Ranjan)

**Note:** However, the author may reproduce or authorize others to reproduce material extracted verbatim from the thesis or derivative of the thesis for author's personal use provided that the source and the Institute's copyright notice are indicated.

**Dedicated to my parents,  
extended family, and all my  
mentors**

## Acknowledgment

Completing PhD has always been a long and rewarding journey that would not be possible without the support, guidance, and encouragement of many individuals. As this enthralling journey comes close to earning my PhD, I would like to thank everyone who has supported me along the way. I would be grateful to the Indian Institute of Technology (BHU) Varanasi, India, and its department, the School of Biochemical Engineering, for providing me with opportunities and the best facilities to carry out my doctoral studies. I would like to express my deepest gratitude to my supervisor, **Prof. Vikash Kumar Dubey**, for his invaluable guidance, insightful feedback, unwavering support, and strong sense of work ethic throughout my research. His patience, knowledge, and dedication were crucial in helping me navigate through the challenges of this work. I am also profoundly thankful to other members of my doctoral committee, **Dr. Prodyut Dhar** and **Prof. Rajesh Kumar Upadhyay**, for their thoughtful suggestions, constructive criticism, and encouragement.

I am also thankful to **Prof. Sayam Sunder, IMS, BHU**, and his group for providing me murine macrophages (J774 A1) cell lines and also **Dr. Rakesh Kumar Singh, Department of Biochemistry, BHU**, and his student for providing me leishmanial culture and valuable suggestions. I am also thankful to the administrative and technical staff of the **Paramshivay supercomputing system**, who sincerely helped me with their facilities during the COVID-19 pandemic. I would also like to acknowledge the administrative and technical staff of CIF, IIT(BHU), CDC, SATHI, BHU, and ISLS, BHU, for their assistance and for ensuring that everything ran smoothly during my experiment.

I am fortunate and also grateful to have had a chance to meet and work with many outstanding seniors like **Dr. Sunita Yadav, Dr. Subhomoy Borkotoky, Dr. Jay Prakash Yadav, Dr. Monu Pande, and Dr. Debanjan Kundu**, who helped me in my research work and also various way throughout my PhD journey. I am thankful to my other lab members, **Dr. Kumari Prerna, Dr.**

**Ehasanullah Khan, Mr. Manash Sarma, Ms. Naveena Menpadi, Mr. Kushal Bora, Mr. Shiv Kaliya, and Ms. Senha Kataria** for their support and co-operation in the lab.

I owe my special thanks to my other friends like **Shikha Rani, Darshna, Divya, Supartim Mahapatra, Rahul Ranjan, and Rohit Rai**, who have always motivated and helped me in difficult times.

I am deeply grateful to **CSIR-UGC** and the **Prime Minister Research Fellowship** for providing the financial support that enabled me to pursue my research without financial burden.

On a personal note, I wish to extend my heartfelt thanks to **my parents** for their unconditional love, endless patience, and unwavering belief in my potential, as well as to **my siblings** for their encouragement and understanding.

Thank you all.

**Preeti Ranjan**

**July, 2024**

## List of Abbreviations

TCA	Tricarboxylic Acid
VL	Visceral
CL	Cutaneous
MCL	Mucocutaneous
FDA	Food and Drug Administration
WHO	World Health Organization
AMR	American Region
AFR	African Region
EMR	Eastern Mediterranean Region
SEAR	South-East Asia Region
SbV	Pentavalent Antimony
Sb+3	Trivalent Antimony
AQP1	Aquaporin 1
ABC	ATP-binding Cassette
AmB	Amphotericin B
HIV	Human Immunodeficiency Virus
ABCC3	ATP binding Cassette Subfamily C Member 3
SSG	Sodium Stibogluconate
PR	Paromomycin
RNS	Reactive Nitrogen Species
ROS	Reactive Oxygen Species
NADH	Nicotinamide Adenine Dinucleotide
Acetyl-CoA	Acetyl Coenzyme A
FADH2	Flavin Adenine Dinucleotide
ETC	Electron Transport Chain
IDH	Isocitrate Dehydrogenase
OGDC	oxoglutarate dehydrogenase complex
SCS	Succinyl-CoA synthetase

GDP	Guanosine Diphosphate
GTP	Guanosine Triphosphate
ATP	Adenosine Triphosphate
CS	Citrate synthase
CIC	Citrate Carrier
ACC	Acetyl CoA Carboxylase
NAD	Nicotinamide Adenine Dinucleotide (oxidized form)
OXPPOS	Oxidative Phosphorylation
PK	Pyruvate Kinase
PFK1	Phosphofructokinase-1
FBPase1	Fructose 1,6-bisphosphatase
FBPase2	Fructose 2,6-bisphosphatase
PFK2	Phosphofructokinase-2
PDH	Pyruvate Dehydrogenase
SDH	Succinate Dehydrogenase
ACLY	ATP Citrate Lyase
FAO	Fatty Acid Oxidation
CPT1	Carnitine Palmitoyl Transferase 1
IFN- $\gamma$	Interferon Gamma
NF- $\kappa\beta$	Nuclear Factor Kappa B
PGE2	Prostaglandin E2
NO	Nitric Oxide
HIF-1 $\alpha$	Hypoxia-Inducible Factor 1-Alpha
IL-1 $\beta$	Interleukin 1 Beta
FASN	Fatty Acid Synthase
TLR4	Toll-like Receptor 4
LTB4	Leukotriene B4
iNOS	Inducible Nitric Oxide Synthase
NRF2	Nuclear Factor Erythroid 2- related Factor 2 f
ATF3	Activating Transcription Factor 3

TNF $\alpha$	Tumor Necrosis Factor Alpha
IFN $\beta$	Interferon Beta
GSH	Glutathione
KEAP1	Kelech-like ECH Associated Protein 1
ACSS	Acetyl-CoA Synthetase
DC	Dendritic Cell
NTDs	Neglected Tropical Diseases
LdCS	<i>Leishmania donovani</i> citrate synthase
MMPBSA	Molecular Mechanics Poisson- Boltzmann Surface Area
ADMET	Adsorption-Distribution- Metabolism- Excretion- Toxicity
MD Simulation	Molecular Dynamic Simulation
NCBI	National Centre for Biotechnology Information
I-TASSER	Iterative Threading Assembly Refinement
RCSB PDB	Research Collaboratory for Structural Bioinformatics Protein Data Bank
C Score	Confidence Score
Tm Score	Template Modelling Score
SDF	Spatial Data File
PDBQT format	Protein Data Bank, Partial Charge, Atom Type format
LGA	Lamarckian Genetic Algorithm
NVT	Number of particles, system Volume, and Temperature
NPT	Number of particles, system Pressure, and Temperature
PME	Particle Mesh Ewald
RMSD	Root Mean Square Deviation
RMSF	Root Mean Square Fluctuation
H-bond	Hydrogen Bond
Rg	Radius of Gyration
PB	Poisson- Boltzmann
SASA	Solvent Accessible Surface Area
HsCS	Human Citrate Synthase
CNS	Central Nervous System

CYP	Cytochrome Protein
hERG	Human Ether-a-go-go-Related Gene
BBB	Blood Brain Barrier
VDs	Volume of Distribution
MRTD	Maximum Recommended Tolerated Dose
CD	Circular Dichroism
GnHCl	Guanidine Chloride
PMSF	Phenyl Methyl Sulfonyl Fluoride
ANS	8-Anilionnaphthalene-1-sulphonic acid
PCR	Polymerase Chain Reaction
NaCl	Sodium Chloride
KCl	Potassium Chloride
SDS-PAGE	Sodium Dodecyl Sulphate Poly Acrylamide Gel Electrophoresis
BSA	Bovine Serum Albumin
K <sub>sv</sub>	Stern-Volmer quenching constant
Ni-NTA	Nickel- Nitrilo Tri Acetic Acid
KI	Potassium Iodide
RPE	Ribulose-5-Phosphate Epimerase
T <sub>m</sub>	Melting Temperature
K <sub>i</sub>	Inhibition Constant
HR <sup>+</sup>	Hormone Receptor-Positive
HER2 <sup>-</sup>	Human Epidermal growth factor Receptor negative
CDK4 & 6	Cyclin Dependent Kinase 4 & 6
SERM	Selective Estrogen Receptor Modulator
PAR-1	Protease Activated Receptor -1
TK	Tyrosine Kinase
H2DCFDA	2',7'- Dichloro Dihydro Fluorescein Diacetate
M199	Medium 199
RPMI 1640	Rosewell Park Memorial Institute 1640
FBS	Fetal Bovine Serum

DMSO	Dimethyl Sulfoxide
DTNB	5, 5-Dithio-bis-(2-Nitrobenzoic acid)
TNB	5-thio-2-nitrobenzoate
OAA	Oxaloacetic acid
NaOH	Sodium Hydroxide
K <sub>m</sub>	Michalis-Menten Kinetics Constant
K <sub>cat</sub>	Catalytic Constant
MTT	3-(4, 5- dimethyl thiazolyl-2)-2,5-diphenyltetrazolium bromide
PBS	Phosphate Buffer Saline
IC <sub>50</sub>	Half-maximal Inhibitory Concentration
EC <sub>50</sub>	Half-maximal Effective Concentration
CC <sub>50</sub>	Cytotoxic Concentration
SI	Selectivity Index
ANOVA	Analysis of Variance
SEM	Standard Error of the Mean
K <sub>b</sub>	Binding Constant
MitoSOX	Mitochondrial Superoxide
DAPI	Diamidino-2-phenyl Indole
PI	Propidium Iodide
CCCP	Carbonyl cyanide 3-chlorophenylhydrazone
SDS	Sodium dodecyl Sulfate
EDTA	Ethylenediamine tetra acetic Acid
SEM	Scanning Electron Microscope
JC-1	5,5,6,6'- tetrachloro-1,1',3,3' tetraethylbenzimidazolylcarbocyanine iodide

## List of Tables

**Table 1. 1:** Risk factors of emergence and re-emergence of leishmaniasis and their effects.

**Table 1. 2:** Currently available antileishmanial drug and their related information.

**Table 2.1:** Natural compound showing free binding energy (kcal/mol) with LdCS & HsCS and its current application.

**Table 2.2:** Analysis of pharmacokinetics properties of ligands, i.e., Staurosporine, Solasodine, Cromolyn, and Oxetacaine, that had been predicted by the pkCSM server.

**Table 2.3:** Calculation of average binding energy of different complexes, i.e., Staurosporine, Solasodine, Cromolyn, and Oxetacaine with Ld citrate synthase after MD simulation.

**Table 2.4:** FDA-approved Ligand showing free binding energy (kcal/mol) with LdCS and HsCS and inhibitor constant (K<sub>i</sub>) with LdCS.

**Table 2.5:** Analysis of Lipinski rule of Ligand.

**Table 2.6:** ADMET properties analysis of ligands along with the known drugs Miltefosine as a control.

**Table 2.7:** Calculation of average binding energy of different complexes with Ld citrate synthase after MD simulation.

**Table 3.1:** Secondary structure contents of the LdCS at different pH.

**Table 4.1:** Kinetics Parameters of *Leishmania donovani* citrate synthase.

**Table 4.2:** Kinetic studies of inhibitor with LdCS in the presence of substrate Acetyl-CoA and Oxaloacetic acid by keeping one substrate constant at a time.

**Table 4.3:** Antileishmanial activity and selectivity index of Abemaciclib, Bazedoxifene, Vorapaxar, and Imatinib on promastigote & Intra-macrophagic amastigotes as well as their Cytotoxicity effect on the murine macrophages cell line J774A.1.

## List of Figures

**Figure 1.1:** Life Cycle of Leishmania and its stages

**Figure 1.2:** Life stages of Leishmania

**Figure 1.3:** Different types of Leishmaniasis

**Figure 1.4:** Worldwide distribution of Cutaneous & Visceral Leishmaniasis

**Figure 1.5:** Central carbon metabolism of Leishmania promastigotes (insect stage) and amastigote (macrophage host)

**Figure 1.6:** Biochemical role of the TCA cycle intermediates

**Figure 1.7:** Crystal structure of Pig heart citrate synthase with labeled angle and dihedral measurements

**Figure 1.8:** Mechanism of Citrate synthase enzyme

**Figure 1.9:** Role of Citrate in cellular metabolism

**Figure 1.10:** Role of Citrate in inflammation

**Figure 1.11:** Drug discovery and repositioning pathways

**Figure 2.1:** *Leishmania donovani* Citrate synthase (LdCS) model and its validation using PROCHECK, RAMPAGE, and ProSA server

**Figure 2.2:** Binding site residues of LdCS and HsCS

**Figure 2.3:** Interaction of compounds with LdCS

**Figure 2.4:** Molecular Dynamic Simulation analysis of LdCS and Complexed compounds

**Figure 2.5:** Hydrogen bond analysis

**Figure 2.6:** Binding energy contribution of complexes

**Figure 2.7:** Interaction of Protein-ligand complexes

**Figure 2.8:** Molecular Dynamic Simulation analysis of LdCS and Complexed ligands, i.e., Imatinib, Bazedoxifene, Vorapaxar, Amyral, and Abemaciclib that performed for 100 ns of time duration

**Figure 2.9:** Hydrogen bond analysis

**Figure 2.10:** The Free binding energy contribution analysis of complexes

**Figure 3.1:** Cloning, Expression, and Purification of *Leishmania donovani* Citrate synthase (LdCS)

**Figure 3.2:** CD spectra of LdCS at varying pH and temperature

**Figure 3.3:** Fluorescence emission spectra of LdCS

**Figure 3.4:** Intrinsic fluorescence quenching of LdCS

**Figure 3.5:** Intrinsic fluorescence unfolding studies of LdCS

**Figure 4.1:** Binding association of selected compound with the LdCS

**Figure 4.2:** Kinetics studies of LdCS

**Figure 4.3:** Inhibition studies with selected compound

**Figure 4.4:** Inhibition studies with selected compound

**Figure 4.5:** The dose-dependent antileishmanial effect of selected compounds such as Abemaciclib, Bazedoxifene, Vorapaxar, and Imatinib on promastigote stage

**Figure 4.6:** The dose-dependent antileishmanial effect of selected compounds such as Abemaciclib, Bazedoxifene, Vorapaxar, and Imatinib on Intra-macrophagic amastigote stage of *Leishmania donovani*

**Figure 4.7:** The Cytotoxic effect of selected compounds on murine macrophages J774 A.1

**Figure 5.1:** Chemical structure of Abemaciclib

**Figure 5.2:** SEM micrograph of morphological changes induced by different concentrations of abemaciclib in *L. donovani*

**Figure 5.3:** The phase contrast and fluorescence microscopy images of untreated and treated promastigote

**Figure 5.4:** Abemaciclib-induced ROS production in promastigote

**Figure 5.5:** Abemaciclib-induced depolarization of mitochondrial membrane potential in promastigote

**Figure 5.6:** The images of promastigote after 48 h exposure of  $IC_{50}$  and  $2x IC_{50}$  concentration of Abemaciclib and stained with DAPI, examined by Phase contrast and fluorescence microscopy at x60

**Figure 5.7:** Cell cycle analysis and Genomic DNA fragmentation assay with Abemaciclib treated sample of promastigote.

**Figure 5.8:** Abemaciclib-induced apoptosis-like cell death in promastigote

## Table of Contents

<b>Contents</b>	<b>page no.</b>
<b>Chapter 1</b>	<b>1</b>
<b>Review of Literature on Leishmaniasis: Introduction, Current Scenario and Future Prospect</b>	<b>1</b>
Abstract	1
1.1 Introduction	2
1.2 Leishmania: the discovery	3
1.3 Life-cycle of Leishmania	6
1.3.1 Promastigote stage	6
1.3.2 Amastigote stage	7
1.4 Types of Leishmaniasis	7
1.5 Distribution of leishmaniasis (worldwide & India)	10
1.6 Risk factors associated with Leishmaniasis	13
1.7 Current therapeutic approach and their drawbacks	15
1.8 The current problem associated with Treatment failure	17
1.9 Outline of promastigote and amastigote metabolism	21
1.10 Tricarboxylic acid cycle (TCA cycle): An antileishmanial drug target	23
1.11 Citrate synthase	25
1.11.1 Structure of citrate synthase	26
1.11.2 Stereochemistry and Mechanism of enzyme	28
1.11.3 Function of Citrate synthase	29
1.11.3.1 In cellular metabolism	28
1.11.3.2 In inflammation as inflammatory signal	32
1.11.3.3 Acetylation of Histones and Non-histone proteins	35
1.12 Drug Repurposing: An Emerging approach in Drug Discovery	36
1.13 Scope of current approach and objective	37
<b>Chapter 2</b>	<b>40</b>
<b>Modelling of <i>Leishmania donovani</i> citrate synthase and virtual screening of compounds using different databases</b>	<b>40</b>
Abstract	40
2.1 Introduction	41
2.2 Materials & Methods	42

2.2.1 Modelling of Citrate synthase and its validation	42
2.2.2 Ligand Preparation	43
2.2.3 Active site prediction	43
2.2.4 Molecular docking and its analysis	43
2.2.5 ADME analysis	44
2.2.6 Molecular dynamic simulation and its analysis	44
2.3 Results	45
2.3.1 Modelled Structure Prediction and its validation	45
3.3.2 Active site Prediction	46
2.3.3 <i>In silico</i> studies with Natural compound database	49
2.3.3.1 Molecular docking and its analysis	49
2.3.3.2 Pharmacokinetics analysis	51
2.3.3.3 Molecular dynamic simulation and its analysis	54
2.3.4 In silico studies with FDA-approved compound database	60
2.3.4.1 Molecular docking for prediction of efficient inhibitor against Ld citrate synthase	60
2.3.4.2 ADME analysis	63
3.3.3.3 Molecular Dynamic Simulation analysis	67
2.4 Discussion	72
2.5 Conclusion	75
<b>Chapter 3</b>	<b>76</b>
<b>Validation of <i>Leishmania donovani</i> citrate synthase as drug target through biophysical studies</b>	<b>76</b>
Abstract	76
3.1 Introduction	77
3.2 Materials & Methods	78
3.2.1 Materials	78
3.2.2 Molecular Cloning, Expression and Purification of LdCS	79
3.2.3 CD Measurements	80
3.2.4 Intrinsic and Extrinsic Fluorescence studies of LdCS protein at different pH	80
3.2.5 Evaluation of tryptophan position in LdCS protein using Potassium iodide and Acrylamide.	81
3.2.6 Unfolding studies of LdCS protein using Urea and Guanidine Chloride.	81
3.3 Results	82
3.3.1 Cloning, expression, and purification of <i>Leishmania donovani</i> Citrate synthase	82

3.3.2 Determination of the secondary structure of LdCS and its thermal stability	83
3.3.3 Intrinsic and extrinsic fluorescence analysis of LdCS at different pH	84
3.3.4 Assessment of tryptophan location in LdCS protein using Potassium Iodide and Acrylamide.	86
3.3.5 Urea and Guanidine Chloride-induced unfolding studies of LdCS protein	87
3.4 Discussion	89
3.5 Conclusion	91
<b>Chapter 4</b>	<b>93</b>
<b>Evaluation of selected compound as potential inhibitor of citrate synthase: an alternative chemotherapeutic option against leishmaniasis.</b>	<b>93</b>
Abstract	93
4.1 Introduction	94
4.2 Materials & Methods	95
4.2.1 Materials	95
4.2.2 <i>L. donovani</i> and J774 A.1 cell culture maintenance	95
4.2.3 Intrinsic fluorescence measurement of selected compounds.	96
4.2.4 Enzymatic assay and kinetics studies of LdCS	96
4.2.5 Inhibition studies of LdCS	97
4.2.6 Promastigote viability assay	97
4.2.7 Intra-macrophagic amastigotes viability assay	98
4.2.8 Cell toxicity assay in J774A.1 macrophage	98
4.2.9 Statistical analysis	99
4.3 Results	99
4.3.1 Analysis of the interaction of the selected compound with <i>L. donovani</i> citrate synthase by fluorescence spectroscopy	99
4.3.2 Kinetic characterization of <i>L. donovani</i> citrate synthase activity	101
4.3.3 Analysis of inhibition kinetics of <i>L. donovani</i> citrate synthase	102
4.3.4 Effect of the selected compound on promastigote viability	104
4.3.5 Effect of selected compounds on intra-macrophagic amastigote viability	107
4.3.6 Cytotoxic effect of the selected compound on J774A.1 cell lines.	108
4.4 Discussion	111
4.5 Conclusion	112
<b>Chapter 5</b>	<b>114</b>
<b>Deciphering molecular mechanism of anticancer compound abemaciclib on underlying antileishmanial activities.</b>	<b>114</b>

Abstract	114
5.1 Introduction	115
5.2 Materials & Methods	116
5.2.1 Materials	116
5.2.2 <i>L. donovani</i> and J774 A.1 cell culture maintenance	116
5.2.3 Morphological analysis of promastigote	117
5.2.4 Analysis of mitochondrial integrity of promastigote	117
5.2.5 Analysis of ROS generation in promastigote	117
5.2.6 Analysis of mitochondrial membrane potential in promastigote	118
5.2.7 Detection of chromatin condensation in promastigote	118
5.2.8 DNA Laddering assay in promastigote	119
5.2.9 Cell cycle analysis in promastigote	119
5.2.10 Determination of phosphatidylserine exposure and membrane integrity in promastigote	120
5.2.11 Statistical analysis	120
5.3 Results	120
5.3.1 Morphological analysis of Abemaciclib treated promastigote	120
5.3.2 Analysis of effect of Abemaciclib on mitochondrial integrity of promastigote	120
5.3.3 Abemaciclib induced ROS production in Promastigote	122
5.3.4 Abemaciclib induced depolarization of mitochondrial membrane potential in promastigote	123
5.3.5 Analysis of effect of Abemaciclib on nuclear structure of promastigote	124
5.3.6 Abemaciclib induced cell cycle changes in promastigote	125
5.3.7 Abemaciclib induced Genomic DNA fragmentation	126
5.3.8 Abemaciclib induced externalization of phosphatidylserine in the plasma membrane of promastigote	126
5.4 Discussion	127
5.5 Conclusion	129
<b>Chapter 6</b>	130
<b>Summary and Future aspects</b>	130
<b>References</b>	137
<b>APPENDIX A</b>	152
LIST OF PUBLICATION & PATENT	152
<b>APPENDIX B</b>	153
CONFERENCES & WORKSHOPS	153

## Abstract

Leishmaniasis, a neglected tropical disease caused by various species of *Leishmania*, presents a significant global health challenge, especially in tropical and subtropical regions like Latin America, Southeast Asia, and parts of Africa. Annually, there are 700,000 to 1 million new cases, and 25,000 to 26,000 deaths occur worldwide. Factors like climatic shifts, co-infections with diseases such as HIV, and population mobility have altered its distribution, exacerbating its impact. It is also termed a "poverty-associated disease" due to its prevalence among economically disadvantaged populations with limited healthcare access and minimal influence on government policies. Current treatment options are inadequate, marked by several issues such as toxicity, high cost, complex administration, and drug resistance. The pharmaceutical industry's lack of focus on this disease further hampers the development of innovative therapeutics, underscoring the need for new drug targets and the repurposing of existing drugs.

Amastigotes of *Leishmania*, which reside in the phagolysosomes of host cells, endure low pH, high temperatures, and oxidative stress, often entering a semi-quiescent state to evade host defences. They primarily utilize sugars and fatty acids for survival and growth, with the TCA cycle playing a crucial role in their metabolic pathways. Citrate synthase (CS), the first enzyme of the TCA cycle, was identified as a potential drug target due to its pivotal role in the continuation of the TCA cycle & energy production in mitochondria and cholesterol & fatty acid synthesis.

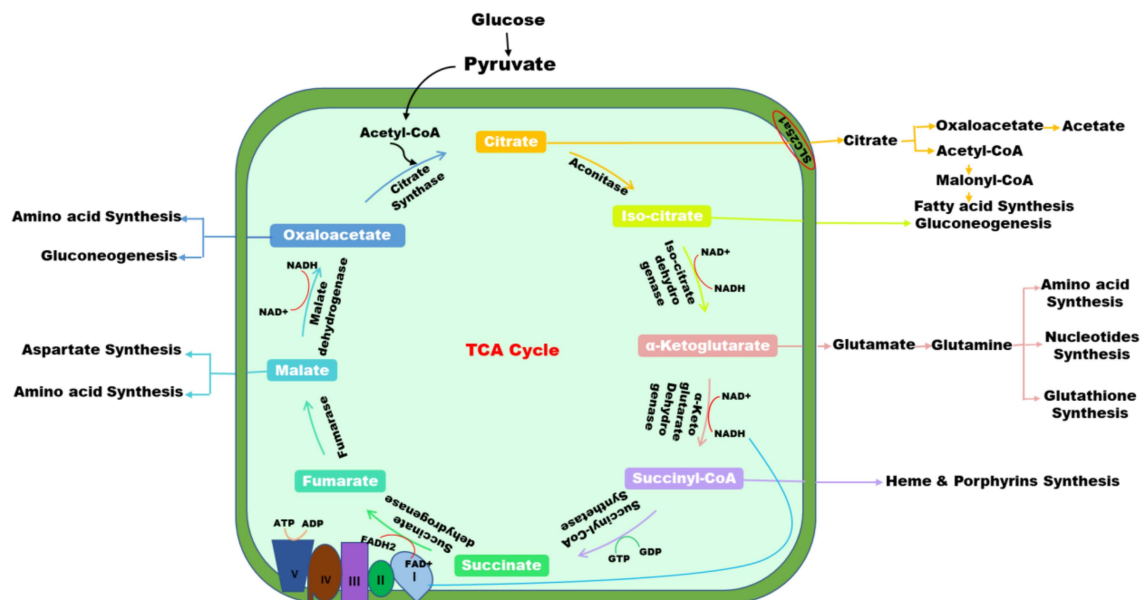


Figure 1: Biochemical role of TCA cycle intermediate.

in the cytosol and significant structural and sequential differences from the human version, making it a viable candidate for selective drug targeting.

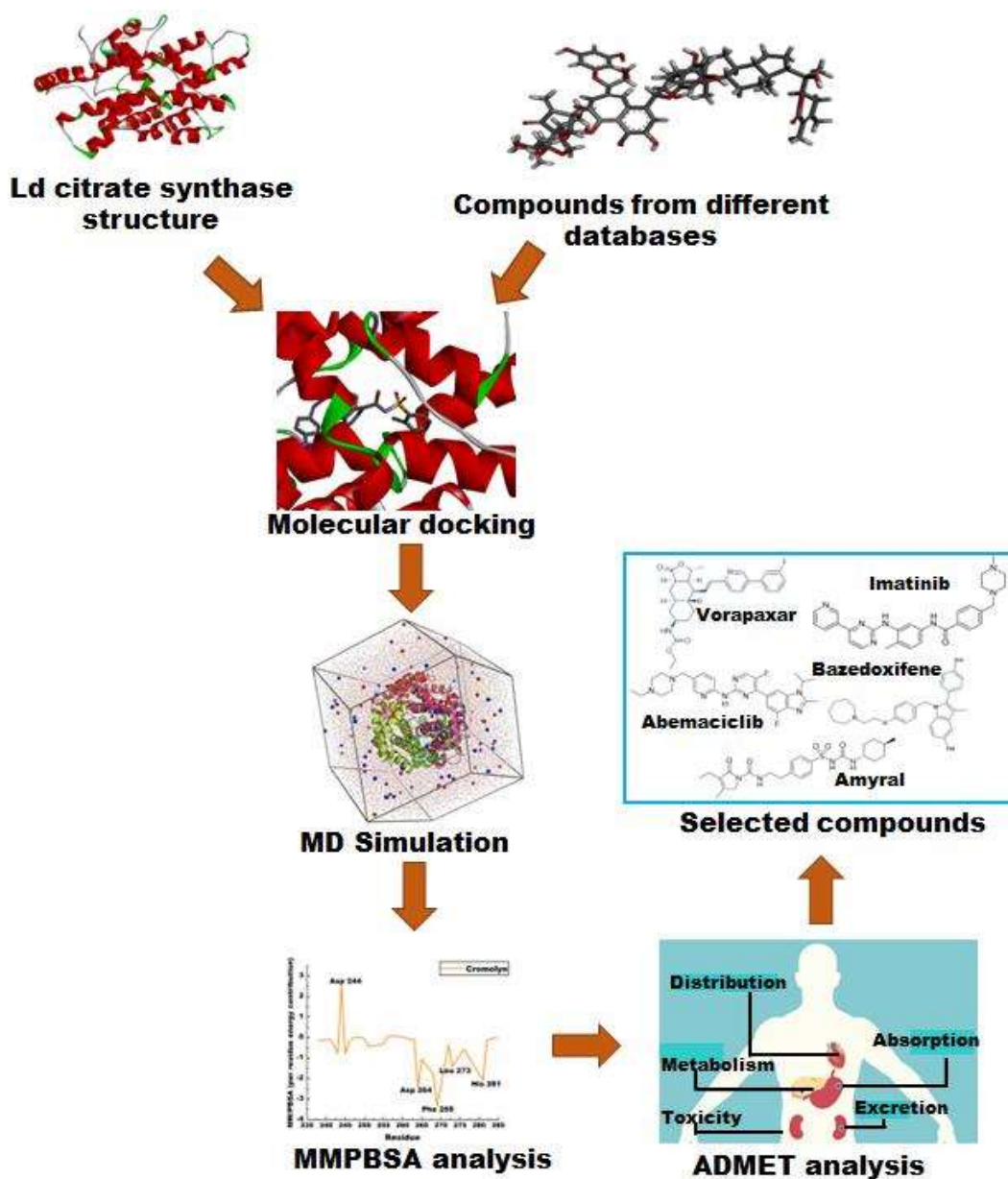
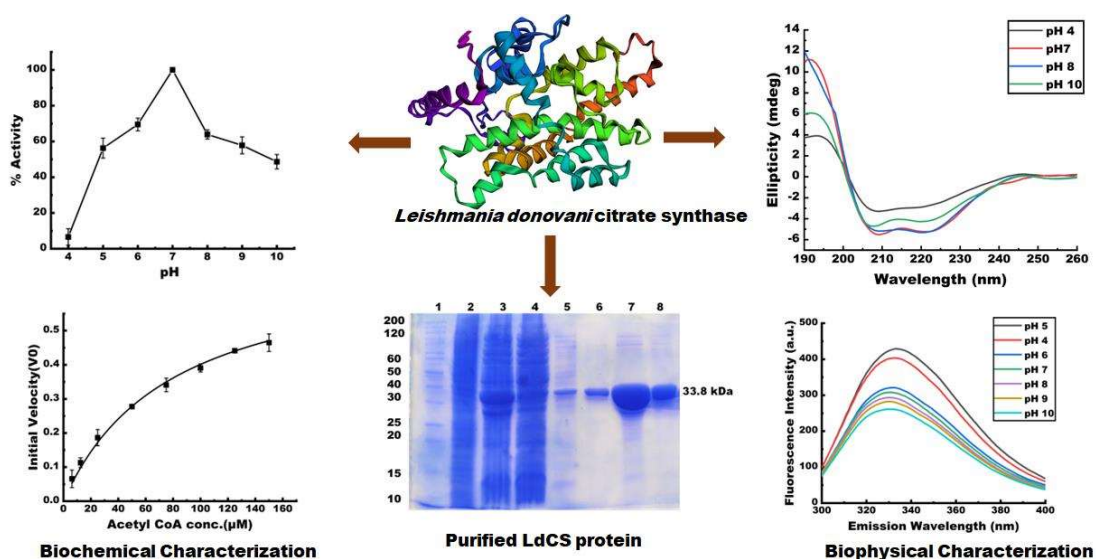


Figure 2: *In silico* studies for selecting top hits using LdCS as a drug target.

In this study, the crystal structure of *Leishmania donovani* citrate synthase (LdCS) was not available; thus, a model was generated using the ITASSER server. The best model, based on C and TM scores, was energy minimized and validated using RAMPAGE and ProSA servers. This validated model was used for molecular docking studies with 1065 natural and 1565 FDA-

approved compounds from the ZINC 15 database. The top five hits—Abemaciclib, Bazedoxifene, Vorapaxar, Imatinib, and Amyral—were selected based on their lower binding energies with LdCS compared to human citrate synthase (HsCS) and interactions with the active site residues of LdCS which analysed through discovery studio analyser. All selected compounds adhered to Lipinski's rule, indicating favourable oral bioavailability. Molecular dynamics (MD) simulations were conducted with GROMACS to assess the stability of the protein-ligand complexes, considering parameters like RMSD, RMSF, radius of gyration, and hydrogen bond analysis. The simulations demonstrated that the ligands formed stable, robust interactions with LdCS. MM-PBSA analysis further confirmed the lower binding energies of these complexes, predominantly driven by hydrophobic contacts. Residue energy decomposition studies identified key residues—Tyr 238, His 242, His 245, Asp 264, Phe 269, Leu 273, and Asn 285—crucial for ligand interactions. Pharmacokinetic studies based on ADMET (Absorption, Distribution, Metabolism, Excretion, and Toxicity) analysis showed that all selected ligands had good water solubility, strong CaCO-2 permeability, good intestinal absorption, and minimal toxicity. These properties suggest favourable pharmacokinetic profiles and potential for effective therapeutic application.



**Figure 3: Biochemical and Biophysical characterization of LdCS.**

To further characterize LdCS, biophysical and biochemical studies were performed. The Ldcs gene was cloned and expressed in a bacterial system, and its protein, purified through affinity chromatography, was confirmed to be pure and of the correct size via SDS-PAGE. Circular dichroism fluorescence spectroscopy revealed that LdCS is predominantly alpha-helical and

maintains a highly folded structure at physiological pH, with changes in secondary structure at extreme pH levels. Thermal denaturation studies indicated that LdCS resists structural changes upon unfolding, with a melting temperature of  $44 \pm 0.31^\circ\text{C}$ . Fluorescence spectroscopy also indicated that LdCS contains tryptophan residues buried in its core, which are sensitive to environmental changes. Quenching studies with potassium iodide and acrylamide confirmed that these residues are accessible to quenchers, suggesting their strategic location within the protein structure. Urea and GnHCl-mediated unfolding studies provided insights into the stability of LdCS, with transition concentrations indicating a relatively stable protein structure. Functional characterization of LdCS included enzyme activity assays, revealing optimal catalytic activity at pH 7.0. Kinetic studies showed a higher  $K_m$  for acetyl-CoA than OAA, indicating a lower affinity for acetyl-CoA.

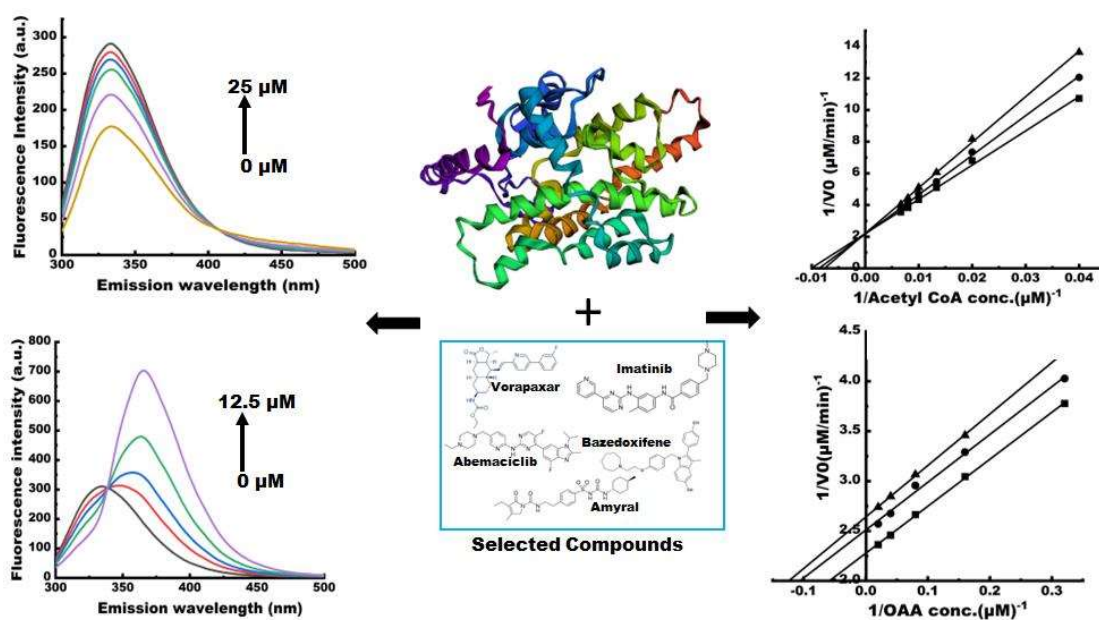


**Figure 4:** *In vitro* studies with selected compound.

Binding studies with selected compounds through fluorescence spectroscopy show good binding affinity, and inhibition studies with selected compounds demonstrated competitive inhibition for acetyl-CoA and uncompetitive inhibition for OAA, with inhibition constants in the micromolar range. Antileishmanial and cytotoxicity studies on promastigote and amastigote forms of *Leishmania*, as well as murine macrophages, revealed that the selected compounds effectively reduced cell viability and infection rates, with  $IC_{50}$  and  $EC_{50}$  values lower than those of the standard drug Miltefosine.

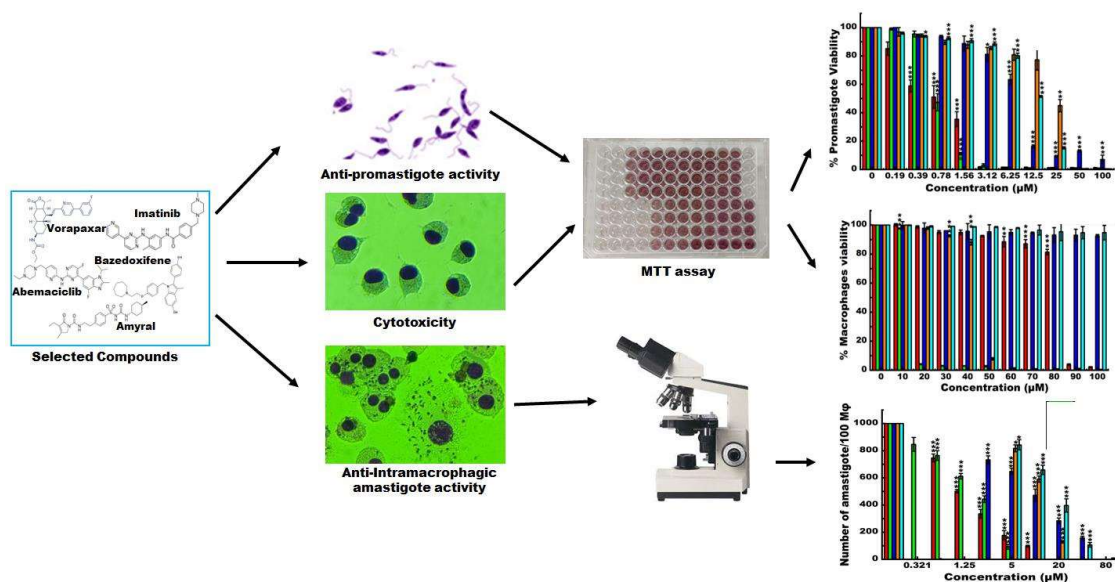


Figure 5: Antileishmanial and cytotoxicity studies with selected compounds.

Vorapaxar showed, till 500  $\mu\text{M}$ , no cytotoxic effects on macrophages, while other compounds exhibited low cytotoxicity, indicating a favourable therapeutic index. Further investigations into the mechanism of action of abemaciclib, based on its potent *in-silico* and *in-vitro* activity, revealed morphological alterations in promastigotes, mitochondrial damage, increased ROS production, depolarization of the mitochondrial membrane, nuclear condensation, increase in Sub G1 cell population in cell cycle assay and DNA fragmentation, indicating its action on mitochondria and an apoptotic mode of death. The apoptotic mode of death was further confirmed with Annexin V and PI, indicating that 64% of cells are in an apoptotic state.

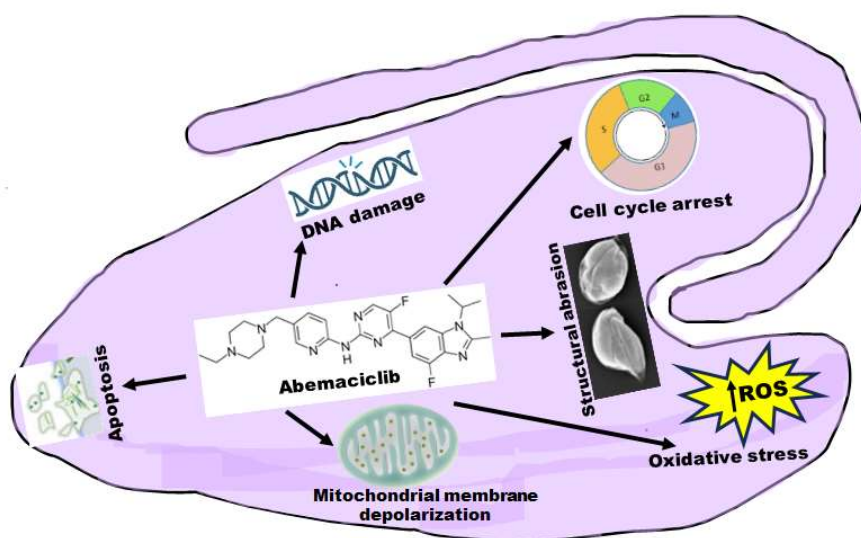


Figure 6: Mode of action of Abemaciclib on *Leishmania donovani*.

These findings suggest that Abemaciclib and other selected compounds are promising therapeutic agents for leishmaniasis, warranting further development and clinical evaluation.